A Biological Interpretation of Transient Anomalous Subdiffusion. I. Qualitative Model

Michael J. Saxton
Department of Biochemistry and Molecular Medicine, University of California, Davis, California

ABSTRACT Anomalous subdiffusion has been reported for two-dimensional diffusion in the plasma membrane and three-dimensional diffusion in the nucleus and cytoplasm. If a particle diffuses in a suitable infinite hierarchy of binding sites, diffusion is well known to be anomalous at all times. But if the hierarchy is finite, diffusion is anomalous at short times and normal at long times. For a prescribed set of binding sites, Monte Carlo calculations yield the anomalous diffusion exponent and the average time over which diffusion is anomalous. If even a single binding site is present, there is a very short, almost artifactual, period of anomalous subdiffusion, but a hierarchy of binding sites extends the anomalous regime considerably. As is well known, an essential requirement for anomalous subdiffusion due to binding is that the diffusing particle cannot be in thermal equilibrium with the binding sites; an equilibrated particle diffuses normally at all times. Anomalous subdiffusion due to barriers, however, still occurs at thermal equilibrium, and anomalous subdiffusion due to a combination of binding sites and barriers is reduced but not eliminated on equilibration. This physical model is translated directly into a plausible biological model testable by single-particle tracking.

INTRODUCTION

In normal diffusion, the mean-square displacement of the diffusing particle is proportional to time, but in anomalous subdiffusion diffusion is hindered and the mean-square displacement is proportional to some power of time <1. As is well known, anomalous diffusion may result from obstruction (1). If the obstacle concentration is below the percolation threshold, diffusion is anomalous at short times and normal at long times. As the obstacle concentration approaches the percolation threshold, diffusion becomes more anomalous for longer times (2). At the percolation threshold, diffusion on the infinite percolation cluster is anomalous over all timescales. It is well known that anomalous diffusion may also result from appropriate distributions of traps. A suitable infinite hierarchy leads to anomalous diffusion at all times; finite hierarchies lead to anomalous diffusion at short times and normal diffusion at long times (3). In the physics literature, anomalous diffusion is often defined to require the diffusion to be asymptotically anomalous, but the case we consider is of interest in biophysical applications and chemical kinetics.

We present here a biological interpretation of anomalous subdiffusion in a finite hierarchy of traps. This interpretation was suggested by the experiments of Platani et al. (4) on three-dimensional anomalous subdiffusion of Cajal bodies in the nucleus, but it is also applicable to two-dimensional diffusion in the plasma membrane and three-dimensional diffusion in the cytoplasm. We show that anomalous subdiffusion in such a system of traps requires the system to be in a nonequilibrium state, so in the biological case metabolic energy is required. The model predicts a crossover from anomalous to normal diffusion. We show that anomalous subdiffusion due to trapping disappears on thermal equilibration, but anomalous subdiffusion due to barriers is unaffected. The initial period of anomalous subdiffusion determines the time required for the first visit of the diffusing particle to its target, so the initial period of anomalous subdiffusion may control reaction kinetics. Quantitative aspects of this model will be discussed in the sequel (M. J. Saxton, unpublished), and later work will apply the model to the experimental data of Platani et al. (4). This work extends previous work (5); preliminary results were presented earlier (6–8). A similar biological interpretation of binding and one-dimensional diffusion of a protein along DNA was proposed independently by Barbi et al. (9,10).

Diffusion is characterized by the time-dependence of the mean-square displacement $\langle r^2 \rangle$. In normal diffusion,

$$\langle r^2 \rangle \propto Dt, \tag{1}$$

where the diffusion coefficient D is constant and t is time. In pure anomalous subdiffusion

$$\langle r^2 \rangle \propto t^{\alpha}, \alpha < 1 \tag{2}$$

at all times, where α is the anomalous diffusion exponent. The diffusion coefficient is therefore time-dependent,

$$D(t) \propto 1/t^{1-\alpha}, \tag{3}$$

appropriately modified to give the proper limit at $t = 0$, say $D(t) = D_0/(1 + t^{1-\alpha})$. The case of interest here is transient anomalous subdiffusion, in which there is a crossover from anomalous subdiffusion at short times to normal diffusion at long times,

Submitted July 3, 2006, and accepted for publication November 6, 2006.

Address reprint requests to M. J. Saxton, Dept. of Biochemistry and Molecular Medicine, University of California, 1 Shields Ave., Davis, CA 95616. Tel.: 530-752-6163; E-mail: mjsaxton@ucdavis.edu.

0006-3495/07/02/1178/14 $2.00

doi: 10.1529/biophysj.106.092619

$$\langle r^2 \rangle \propto \begin{cases} t^{\alpha} & \text{for } t \ll t_{CR} \\ t & \text{for } t \gg t_{CR} \end{cases}, \quad (4)$$

where t_{CR} is the crossover time. A definition of anomalous subdiffusion sometimes used in the physics literature excludes this case by requiring that diffusion be anomalous asymptotically, but instead of defining away the transient anomalous subdiffusion, we analyze and quantify the initial period of anomalous diffusion. Fig. 1 *a* shows $\langle r^2 \rangle$ as a function of time for pure normal diffusion, transient anomalous subdiffusion, and pure anomalous subdiffusion. The structure is apparent in Fig. 1 *b*, a log-log plot of the same data, and is even clearer in the plots actually used to analyze the Monte Carlo data. As shown in Fig. 1 *c*, to emphasize the crossover we remove the asymptotic time dependence and plot log $\langle r^2 \rangle / t$ versus log t, so that anomalous diffusion gives a straight line of slope $\alpha - 1$, normal diffusion gives a horizontal line, and the intersection of these lines gives the crossover time. Here $\langle r^2 \rangle / t$ can be considered to be a time-dependent diffusion coefficient $D(t)$, normalized to 1 for free diffusion. This approach was used to analyze anomalous subdiffusion in obstructed systems as the obstacle concentration approached the percolation threshold (2).

Measurements of anomalous subdiffusion in cells and cell membranes by fluorescence recovery after photobleaching (FRAP), fluorescence correlation spectroscopy (FCS), and single-particle tracking (SPT) are reviewed elsewhere (M. J. Saxton, unpublished).

Fig. 2 shows experimental results from two noteworthy articles, plotted as in Fig. 1 *c*. Platani et al. (4,11) measured the anomalous diffusion of Cajal bodies in the nucleus of HeLa cells. Cajal bodies are small spherical structures of diameter ~0.1–2.0 μm, made up of protein and RNA. Fig. 2 *a* shows these results. In the untreated cells, diffusion is anomalous over 1.5 orders of magnitude in time. Treatment with the transcriptional inhibitor actinomycin D makes diffusion faster and less anomalous. Energy depletion with azide and 2-deoxyglucose makes diffusion faster and reduces the duration of the anomalous period. Quantitative analysis shows that the anomalous subdiffusion exponent α increases from 0.67 for the untreated cells to 0.78 in the azide-treated cells and 0.90 in the actinomycin-treated cells. The authors conclude that both metabolic energy and ongoing transcription are required to maintain activity of the binding sites and obstacles responsible for anomalous subdiffusion. Another noteworthy result is the SPT work of the Kusumi laboratory on the plasma membrane (12). Fig. 2 *b* shows anomalous subdiffusion of gold-labeled dioleoylPE in the plasma membrane of fetal rat skin keratinocyte cells (13). The control, diffusion on blebs (*upper curve*), is normal at all times. In the lower curve, for intact cells, anomalous subdiffusion was observed over three orders of magnitude in time. Values of α are 0.97 for the initial part of the curve, 0.53 for the anomalous region, and 0.94 for the final part. The authors interpret the curve in terms of compartmentation of the

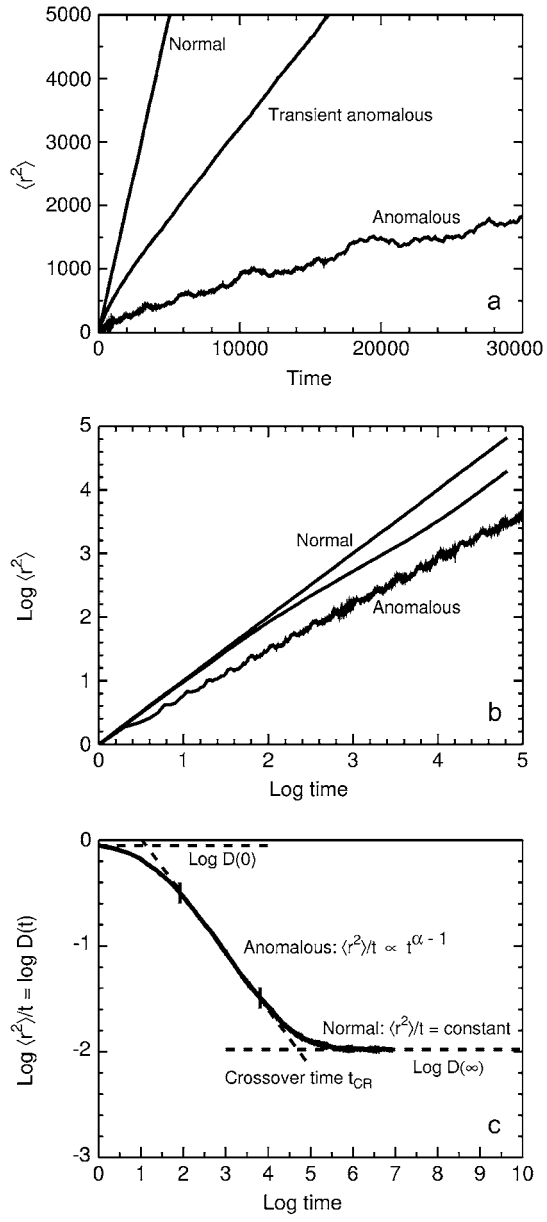

FIGURE 1 Types of diffusion considered. Mean-square displacement $\langle r^2 \rangle$ as a function of time t for normal diffusion, transient anomalous subdiffusion, and pure anomalous subdiffusion. (*a*) Linear plot. (*b*) Log-log plot. Normal diffusion is a random walk on an unobstructed triangular lattice. In notation to be explained later, the transiently anomalous curve is for a hierarchy of traps 8/4/2/– with total trap concentration 14/1024 = 0.01367 and P_{ESC} = 0.1. Pure anomalous subdiffusion is from the Weierstrass-Mandelbrot equation (18) with exponent $\alpha = 0.720$ to match the slope of the power-law part of the transiently anomalous curve. The log-periodicity is an artifact of this function. (*c*) Method of analysis of transient anomalous subdiffusion. The Monte Carlo data is plotted as log $\langle r^2 \rangle / t = \log D(t)$ versus log t. The mean-square displacement is normalized so that $D = 1$ for a system without traps. The initial value is log $D(0)$. The slope of the power-law region yields the anomalous diffusion exponent α; the value in the normal region yields the limiting normal diffusion coefficient log $D(\infty)$; and the intersection of the lines yields the crossover time t_{CR}. The vertical lines mark the power-law region, defined as the region in which the curve is linear to within a few percent. In this plot pure normal diffusion gives a horizontal line and pure anomalous subdiffusion gives a straight line of slope $\alpha - 1$.

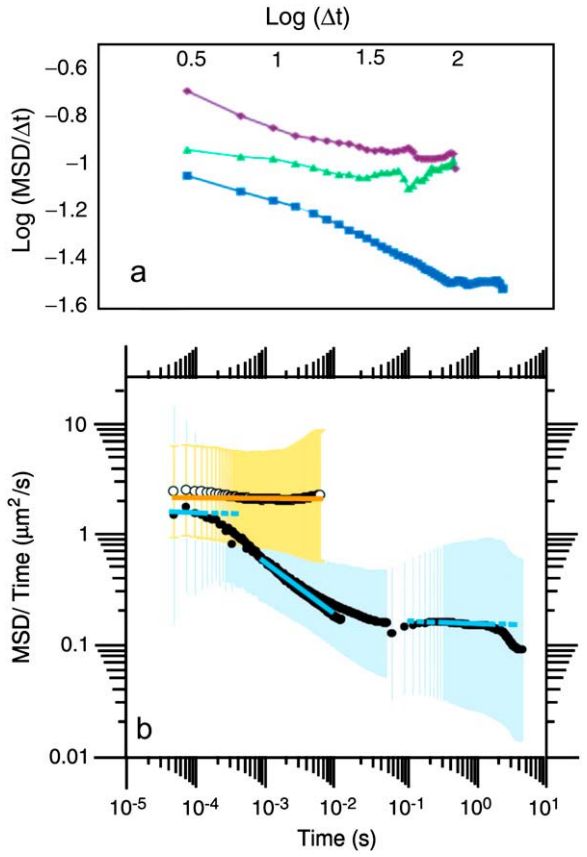

FIGURE 2 Experimental data for the mean-square displacement (MSD) from SPT. Log-log plots of $\langle r^2 \rangle / t$ as a function of time t (or equivalently the lag time Δt). (*a*) Anomalous subdiffusion of Cajal bodies in the nucleus of HeLa cells (4). (*Blue*) Untreated cells. (*Green*) Cells treated with the transcriptional inhibitor actinomycin D. (*Purple*) ATP-depleted cells. (Adapted by permission from Macmillan Publishers Ltd., *Nature Cell Biology*, 4:502–508, copyright 2002.) (*b*) Anomalous subdiffusion of gold-labeled dioleoylPE in fetal rat skin keratinocyte cells (13). (*Upper curve*) Control showing normal diffusion in blebs. (*Lower curve*) Data points obtained at time resolutions of 25 μs, 110 μs, and 33 ms. (*Straight lines*) Least-squares fits to the data; (*blue* and *yellow vertical bars*) standard deviations. (Adapted by permission from *Biophysical Journal*, copyright 2004.)

membrane by actin-based cytoskeletal fences. Their later work shows structure in the anomalous region for the μ-opioid receptor in normal rat kidney fibroblast cells, attributed to nested double compartmentation of the membrane by fences (14). Evidence for the existence of fences from electron tomography is given by Morone et al. (15).

In both cases, the experimental results are consistent with a crossover from anomalous to normal diffusion, although before one could claim this as experimental proof one ought to do simulations to see how much averaging is needed to distinguish a crossover from low-frequency noise.

METHODS

Monte Carlo methods are as described in Saxton (5) except that the ran2 random number generator of Press et al. (16) was used; see also the sequel and (17). Calculations were done on triangular and square lattices in two dimensions and a cubic lattice in three dimensions, with periodic boundary conditions. For each run, at least 50 trap configurations were used, and 200 tracers per trap configuration, except that in Fig. 8, 100 configurations and 500 tracers per configuration were used. The time points were narrowly spaced at small times and widely spaced at large times to provide high resolution without an excessively large data set (18). The runs were highly reproducible. Five independent runs similar to those in the center curve of Fig. 5 were plotted on the same scale as that figure; the total scatter was approximately twice the linewidth. Notation: 1 K = 1024; 1 M = 1024^2. All concentrations are given as number fractions. All energies are in units of kT, where k is Boltzmann's constant and T is temperature.

RESULTS

Infinite hierarchy of binding sites

An appropriate infinite hierarchy of traps is known to give anomalous subdiffusion at all times. If the distribution of escape times t_e is assumed to be a power law with exponent $\beta - 2$,

$$P(t_e)dt_e = (1-\beta)t_e^{\beta-2}dt_e, \beta \in (0,1), \quad (5)$$

then the anomalous diffusion exponent is $\alpha = 1 - \beta$, (19), though in practice correction terms must be included (20). This distribution is so wide that the mean does not exist. An example of the analogous discrete distribution is shown in Table 1. This distribution illustrates the recipe for fractal time of Shlesinger (21): An order-of-magnitude longer escape time, an order-of-magnitude less often. Here at each layer the escape time increases by an order of magnitude in base 3, and the number of traps decreases by an order of magnitude in base 2. Very deep traps are present but are very rare. Note that these infinite hierarchies are inherently nonequilibrium systems. There is no deepest trap so a diffusing particle cannot equilibrate with the traps.

This mechanism is based on permanent traps, but the corresponding distribution of transient traps also gives anomalous subdiffusion. This is the continuous-time random walk (CTRW) model, in which the particle moves at every step but the time required for each move is generated randomly at each step from the distribution of Eq. 5. The escape time from any lattice point thus varies from visit to visit (3). The CTRW is a mean-field version of the trap model in which memory effects are neglected (19).

TABLE 1 Infinite hierarchy of traps

Relative escape time	Relative number of traps
1	1
3	1/2
9	1/4
27	1/8
81	1/16
243	1/32
729	1/64
...	...

Finite hierarchy of binding sites

Monte Carlo calculations show that a finite hierarchy of binding sites is a sufficient condition for anomalous subdiffusion at short times crossing over to normal diffusion at long times. We consider a finite hierarchy obtained by truncating the infinite hierarchy of Table 1, and we take the deepest binding site to be the target site for the diffusing particle. We define traps to be binding sites from which escape is possible, and targets to be reaction sites from which there is no escape and reaction occurs at the first encounter with the target. We can depict the finite hierarchy as in Fig. 3. The binding energy increases by ΔE at each level in the hierarchy. The escape time is given by a Boltzmann factor, so the escape time increases by a factor $\exp(-\Delta E/kT)$ at each level. The energy scale is shown horizontally to emphasize that the diffusing particle is not funneled systematically to the lowest-energy state, as in a model of protein folding (22), but moves randomly among traps and nonbinding sites and has a nonzero probability of reaching the target at the first time step. Thermal equilibration is possible, and the model gives anomalous diffusion at short times and normal diffusion at long times (5). There are no obstacles to diffusion in the model; the traps simply bind and delay the diffusing particle. Typically we assume $P_{\mathrm{ESC}} = 0.1$ so the escape time from the shallowest trap is 10 and $\Delta E/kT = \ln 0.1 = -2.303$. The fundamental quantity describing the effect of the traps is the mean escape time $\langle t_{\mathrm{ESC}} \rangle$. For example, for a single set of 30 traps as in Fig. 3 with $P_{\mathrm{ESC}} = 0.1$ and a total of 1024 sites in the system, we have

$$\langle t_{\mathrm{ESC}} \rangle = [(1024 - 30) \times 1 + (16 \times 10 + 8 \times 10^2 + 4 \times 10^3 + 2 \times 10^4)]/1024 = 25.3457. \quad (6)$$

The limiting diffusion coefficient is then (see Bouchaud and Georges, page 142) (3)

$$D(\infty) = 1/\langle t_{\mathrm{ESC}} \rangle. \quad (7)$$

We show here only Monte Carlo results in which the target site is omitted. These plots give a crossover to normal diffusion at large times, and a clear interpretation of α and the crossover time. When the target site is included, the final square displacement for each diffusing particle is equal to the value when that particle reaches the target. Ultimately, then, the mean-square displacement approaches a constant and the slope of $\log \langle r^2 \rangle / t$ becomes -1, making analysis of the curves less clear.

Fig. 1 *c* shows that a finite hierarchy is a sufficient condition for transient anomalous subdiffusion. Fig. 4 shows what factors increase the duration of the anomalous period and make diffusion more anomalous. In Fig. 4 *a*, as levels are added to the hierarchy at constant P_{ESC} and approximately constant total trap concentration, diffusion is more anomalous for a longer time. The period of anomalous diffusion (in terms of $\log t$) increases from 0.4 to 5.1, and α decreases from 0.92 to 0.33. In Fig. 4 *b*, as P_{ESC} is reduced for a fixed hierarchy and concentration, diffusion is again more anomalous for a longer time. The period of anomalous diffusion increases from 1.0 to 1.5 to 1.9, and α decreases from 0.78 to 0.52 to 0.36. Here the decrease in P_{ESC} corresponds to deepening the traps, not lowering the temperature, because the change in temperature required for a decrease this large would be unphysiological. In Fig. 4 *c*, the trap concentration C is increased for a fixed hierarchy 16/8/4/2/− at fixed $P_{\mathrm{ESC}} = 0.1$. As C increases, diffusion becomes more anomalous for a longer time, primarily on account of the change in $\langle t_{\mathrm{ESC}} \rangle$. Here $\langle t_{\mathrm{ESC}} \rangle$ increases from 25.3457 to 390.5, the period of anomalous subdiffusion increases from 1.6 to 2.6, and α decreases slightly, from 0.53 to 0.44.

In all three plots, if one observed the shallower curves in isolation, one would not count them as power-law curves but simply as curves with an inflection point. But Fig. 4 suggests that even the shallowest curves ought to be viewed as a limiting case of families of curves that can show a significant region of power-law dependence.

The hierarchy of traps is a sufficient condition for transient anomalous subdiffusion, but it is not a necessary condition. Transient anomalous subdiffusion occurs if the number of traps per level is constant, or even if there is only a single level of traps, but the time in which diffusion is anomalous differs. Fig. 5 compares the standard hierarchy 16/8/4/2/− with the uniform distribution 7/7/7/7/− and a single deep

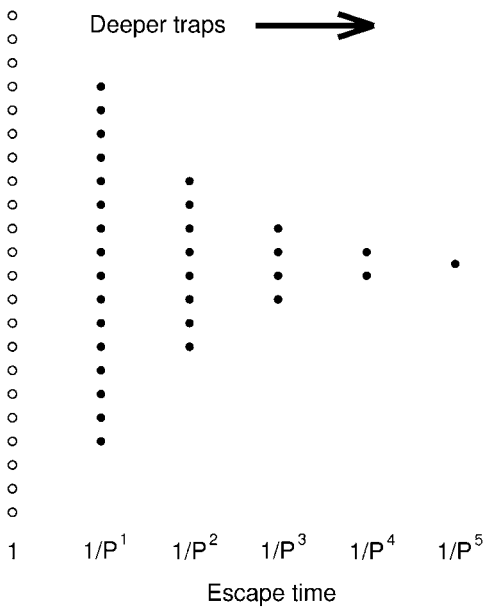

FIGURE 3 Schematic form of a finite hierarchy from truncation of the infinite hierarchy of Table 1. (*Open circles*) Nonbinding sites. (*Solid circles*) Binding sites. As the traps grow deeper, the escape time increases by a factor of $1/P$ at each step, where P is the escape probability per time step from the shallowest traps. This hierarchy will be written as 16/8/4/2/T, where T is the target site, or 16/8/4/2/− when the target site is omitted.

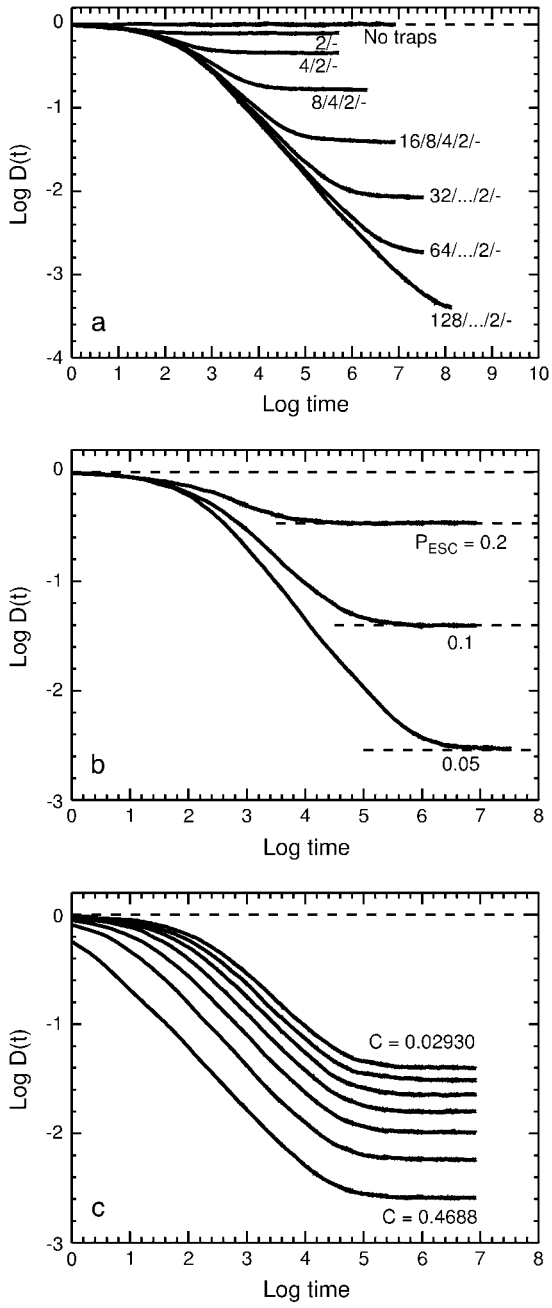

FIGURE 4 A finite hierarchy leads to an initial period of anomalous subdiffusion, followed by a crossover to normal diffusion. Results here are for two-dimensional random walks on a triangular lattice. The corresponding results for square and cubic lattices are very similar. (*a*) Effect of increasing the number of levels in the hierarchy: No traps, 2/−, 4/2/−, 8/4/2/−, 16/8/4/2/−, 32/16/8/4/2/−, 64/. . ./2/−, and 128/. . ./2/−, with $P_{ESC} = 0.1$. One set of traps was used and the system size was varied between 8×8 and 94×94 to keep the total trap concentration as constant as possible. The concentration was 0.02958 ± 0.00096, that is, an SD of 3.26% of the mean. No targets were present. (*b*) Effect of P_{ESC} for a constant hierarchy 16/8/4/2/−. Here $P_{ESC} = 0.2$, 0.1, and 0.05, the trap concentration is $30/1024 = 0.02930$, and the lattice size is 32×32. (*c*) Effect of concentration C for a constant hierarchy 16/8/4/2/−. Here a single set of 30 traps was used, and the lattice edge was set to 32, 28, 24, 20, 16, 12, and 8, giving $C = 0.02930$, 0.03827, 0.05208, 0.07500, 0.1172, 0.2083, and 0.4688, with $P_{ESC} = 0.1$.

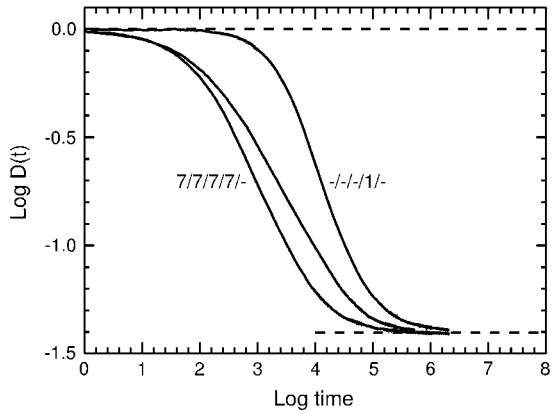

FIGURE 5 Comparison of the effects of a single deep trap, −/−/−/1/−, a four-level set of traps with a fixed number of traps per level, 7/7/7/7/−, and the standard hierarchy 16/8/4/2/−. Here P_{ESC} was set to 0.07958, 0.1364, and 0.1, respectively, so that the mean escape time $\langle t_{ESC} \rangle$ and therefore the limiting value $D(\infty)$ were constant. The lattice size was 32×32. As the traps are varied from the single deep trap to the uniform distribution to the standard hierarchy, the width of the anomalous region increases from 0.82 to 1.29 to 1.79 in units of $\log t$ but diffusion grows less anomalous, with α increasing from 0.23 to 0.44 to 0.54.

trap −/−/−/1/−. Here the total trap concentrations differ but P_{ESC} is adjusted so that $\langle t_{ESC} \rangle$ and $D(\infty)$ are the same for the three distributions of traps. A single trap gives the shortest period of anomalous subdiffusion and the hierarchy gives the longest. The period of power-law dependence for the single deep trap is so short that this case is almost artifactual anomalous subdiffusion, but Figs. 4 and 5 show when the anomalous period becomes significant.

Other models of diffusion in hierarchies

Other models of random walks on discrete hierarchies have been discussed in the physics literature. To describe weakly chaotic motion, Hanson et al. (23) solved a random-walk model for a nearest-neighbor self-similar Markov chain. Here as a particle moves in the hierarchy, the transition rate changes by a constant factor from level to level. Their main result was that the distribution of first passage times for escape from the hierarchy decreases as a power law in t. The essential difference between their model and the model presented in this article is the nature of the random walks. In the model of Hanson et al. (23), the particle carries out a random walk restricted to the hierarchy and moves only to nearest-neighbor levels within the hierarchy. In the trap hierarchy model, the particle moves only to nearest-neighbor lattice sites, but it can move arbitrarily within the hierarchy or to a nonbinding site, depending on what traps happen to be at the nearest-neighbor sites. The interesting similarity is the behavior of the first passage time. As will be discussed in detail in the sequel, we evaluate the first passage time for a particle starting at a random lattice point and carrying out a random walk in the presence of the trap hierarchy until it reaches an

immobile target site. At short times the distribution of first passage times is a power law as in the model of Hanson et al. (23), but at large times there is a crossover to an exponential decay as seen in the trap-free case, though the decay is much slower.

Other work on diffusion in hierarchies examined a regular one-dimensional hierarchy of waiting times (24) or barrier crossing rates (25–27) by renormalization group techniques. Teitel et al. (27) extended the results to random ordering and to two dimensions. In all cases anomalous subdiffusion was found for appropriate values of the parameters, with the mean-square displacement a power of t. But if the well depths or barrier heights form the hierarchy and the jump probabilities are given by the Boltzmann distribution, then the hindrance to diffusion is much more severe. The mean-square displacement is a power of ln t, not t (28). Metzler and Klafter (29) provide a general theoretical context for anomalous subdiffusion due to trapping.

Nonequilibrium state

In a system of traps, a nonequilibrium initial state is a necessary condition for anomalous subdiffusion. Consider the two limits of the initial distribution of diffusing particles. If the particle is initially in a random position, it is in a highly nonequilibrium state because it is at any position with equal probability, whether that position is a nonbinding site or a shallow trap or the target site. But if the particle is initially in thermal equilibrium, it is most likely to be in the deepest trap, that is, at the target site, and in terms of the model the reaction is complete. Table 2 shows an example for a 16/8/4/2/T hierarchy, 30 traps and one target in 1024 lattice points, with the escape probability from the shallowest traps $P_{ESC} = 0.1$ per time step. In this system, for a random state 97% of the diffusing particles are initially at nonbinding sites, but at thermal equilibrium 79% of the particles are initially at the target.

We can think of the nonequilibrium requirement in terms of a time-dependent diffusion coefficient (Eq. 3). For pure anomalous subdiffusion, the diffusion coefficient is initially at some short-range value D_0 and decreases with time, approaching zero at infinite time. But we know that diffusion-mediated processes occur in cells. So if there is to be anomalous diffusion due to a trap mechanism, there must be some biological event that turns on the interaction with the traps and defines $t = 0$, $D(0) = D_0$. There are many possibilities for such an event: changes in localization, such as insertion of a receptor into the plasma membrane or entry of a DNA-binding regulatory protein into the nucleus or assembly of a Cajal body; or conformational change in the diffusing species, such as dimerization of a membrane-bound receptor or binding of a ligand to a receptor or (de)phosphorylation of a protein. Alternatively, the event could turn on or reset the traps rather than the diffusing species.

TABLE 2 Initial position of diffusing particle

	Escape time	Number of sites	Random	Equilibrium
Nonbinding	1	993	0.970	0.0079
	$1/P$	16	0.016	0.0013
	$1/P^2$	8	0.0078	0.0064
	$1/P^3$	4	0.0039	0.032
	$1/P^4$	2	0.00195	0.159
Target	$1/P^5$	1	0.00098	0.794

Note that all of these processes require metabolic energy at some stage of the cycle. The analogous mechanism in a physical system also requires an external energy source to produce anomalous subdiffusion. An amorphous semiconductor has a singular hierarchy of traps for conduction electrons. Anomalous conduction results when a light pulse excites an electron to the conduction band, and the initial position of this electron is independent of the traps in the neighborhood (30).

The most quantitative way of looking at this is a theorem stating that in a random trap model, if the diffusing particle is initially in thermal equilibrium with the traps, then diffusion is normal at all times (31,32) (see Haus and Kehr, 1987, section 7). Diffusion is slow because the mobile particle is most likely to be in the deeper traps and its diffusion rate is determined by the escape time from those traps. But diffusion is normal. This result was confirmed by simulations for the obstruction-binding model, in which some lattice sites contain sticky obstacles (5).

As the diffusing particle equilibrates with the traps, diffusion becomes more normal. Fig. 6 *a* shows the effects of the annealing time on anomalous subdiffusion. If the initial position is random, diffusion is anomalous for a significant time and then crosses over to normal. In the other curves, the diffusing particle is annealed for a prescribed number of time steps before the mean-square displacement is recorded. In the annealed curves, diffusion is first normal, then anomalous, and then normal. As the annealing time increases, the initial period of normal diffusion becomes longer and the period of anomalous diffusion becomes shorter and less anomalous. At very large annealing times, or when the initial position is chosen from an equilibrium distribution, diffusion is slow but normal at all times. Fig. 6 *b* shows that the energy behaves in the same way though the energy crossover times are systematically smaller.

To make clear the range of applicability of these results, we examine a variety of systems of traps and barriers (reviewed briefly in (33–35) and comprehensively in (3,32,36,37); see Ben-Avraham and Havlin, 2000, pages 114–126; and Haus and Kehr, 1987, section 7. We consider the one-dimensional case to examine the results of Barbi et al. (9,10) discussed later. We use random traps and barriers from a continuous distribution to show that the random and discrete cases behave similarly.

In the random site (''valley'') model (38,39) as shown in Fig. 7 *a*, each lattice site is assigned a random binding energy E_i and the diffusing particle must reach $E = 0$ to escape a site. The escape probability $P_i = \exp(-E_i/kT)$ is independent of the final state, and the particle does not know how deep a trap it is entering when it moves to a site. The escape

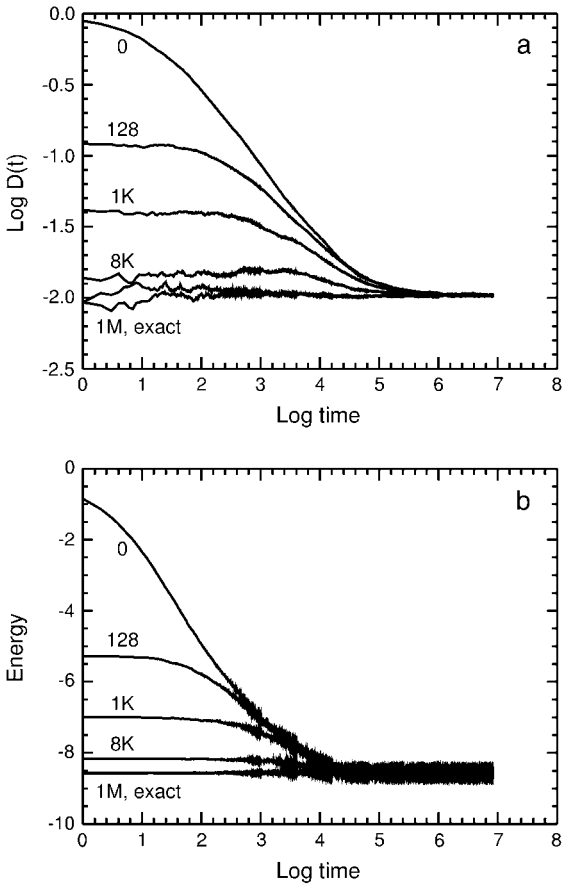

FIGURE 6 Effect of annealing time on a two-dimensional random walk on the triangular lattice. The standard trap hierarchy was used, 16/8/4/2/– with $P_{ESC} = 0.1$, with 1000 sets of traps on a 512×512 lattice, giving a trap concentration of 0.1144. The corresponding plots for random walks on the cubic lattice are very similar. (*a*) Log-log plots of $\langle r^2 \rangle / t$ versus time for various initial conditions. (*b*) Plots of energy versus log time for the same initial conditions. The diffusing particle was placed in a random initial position and annealed for 0, 128, 1 K, 8 K, or 1 M time steps as indicated, or it was placed in a random initial position determined from a Boltzmann distribution (exact). Then the mean-square displacement and energy were recorded. The changes in noise levels are due to changes in the sampling time.

probability is the same in all directions, and there is no correlation between jumps.

In the random bond (''mountain'') model (40–42) shown in Fig. 7 *b*, all sites are at $E = 0$ and random potential energy barriers of height E_{ij} are placed on the bonds between them. The transition probability is symmetric, $P_{ij} = P_{ji} = \exp(-E_{ij}/kT)$, and motion is correlated because a jump over a low barrier is likely to be followed by the reverse jump. At equilibrium the concentration at all sites is the same, so annealing has no effect and transient anomalous diffusion always occurs for a suitable distribution of barriers. Note that in one dimension the tracer cannot avoid a high barrier but in higher dimensions a high barrier has much less effect because the tracer will most likely take a path of lesser resistance and bypass the barrier.

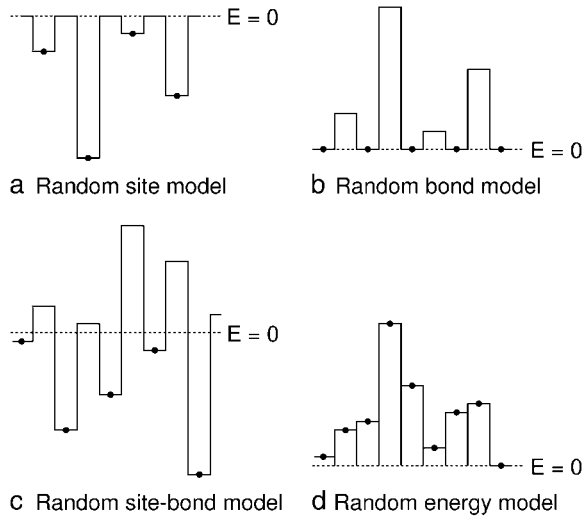

FIGURE 7 Potentials defining the different one-dimensional models. See text for details. Circles represent lattice sites.

In the random site-bond (''mountain-valley'') model (43,44) shown in Fig. 7 *c*, each site is assigned a random binding energy E_i and each bond is independently assigned a random barrier height E_{ij}, not necessarily from the same distribution. The escape probability depends on the initial site depth and the barrier height, but not the final site depth, $P_{ij} = \exp[-(E_i + E_{ij})/kT]$.

In the random energy model (9,10) shown in Fig. 7 *d*, each site is assigned a random energy E_i, and the escape probability is obtained from the Metropolis algorithm,

$$P_{ij} = \begin{cases} 1 & \text{if } \Delta E_{ij} \le 0 \\ \exp(-\Delta E_{ij}/kT) & \text{if } \Delta E_{ij} > 0 \end{cases}, \quad (8)$$

where $\Delta E_{ij} = E_i - E_j$. This is the only model of the four in which the energy of the final state affects the escape probability. Some variants of this model are discussed by Barbi et al. (9,10).

For the random site, site-bond, and energy models, site energies are in general nonzero so the equilibrium distribution of tracers is nonuniform. If the initial position is random, there is an equilibration period. The Monte Carlo results show transient anomalous diffusion when the system is out of thermal equilibrium, and annealing reduces anomalous diffusion as shown in Fig. 6 for the two-dimensional random site model and Fig. 8, *a*, *c*, *d*, and *e*, for the one-dimensional random site, site-bond, and energy models. On equilibration, diffusion in the site model is normal at all times (Fig. 8 *a*) as required by the theorem (31,32) mentioned earlier. In the random site-bond model (Fig. 8 *c*) and the random energy model (Fig. 8, *d* and *e*), anomalous subdiffusion is reduced by annealing but not abolished.

For the random bond model, however, a random initial distribution is the equilibrium distribution, and annealing has no effect, as shown in Fig. 8 *b*. Even if the initial distribution

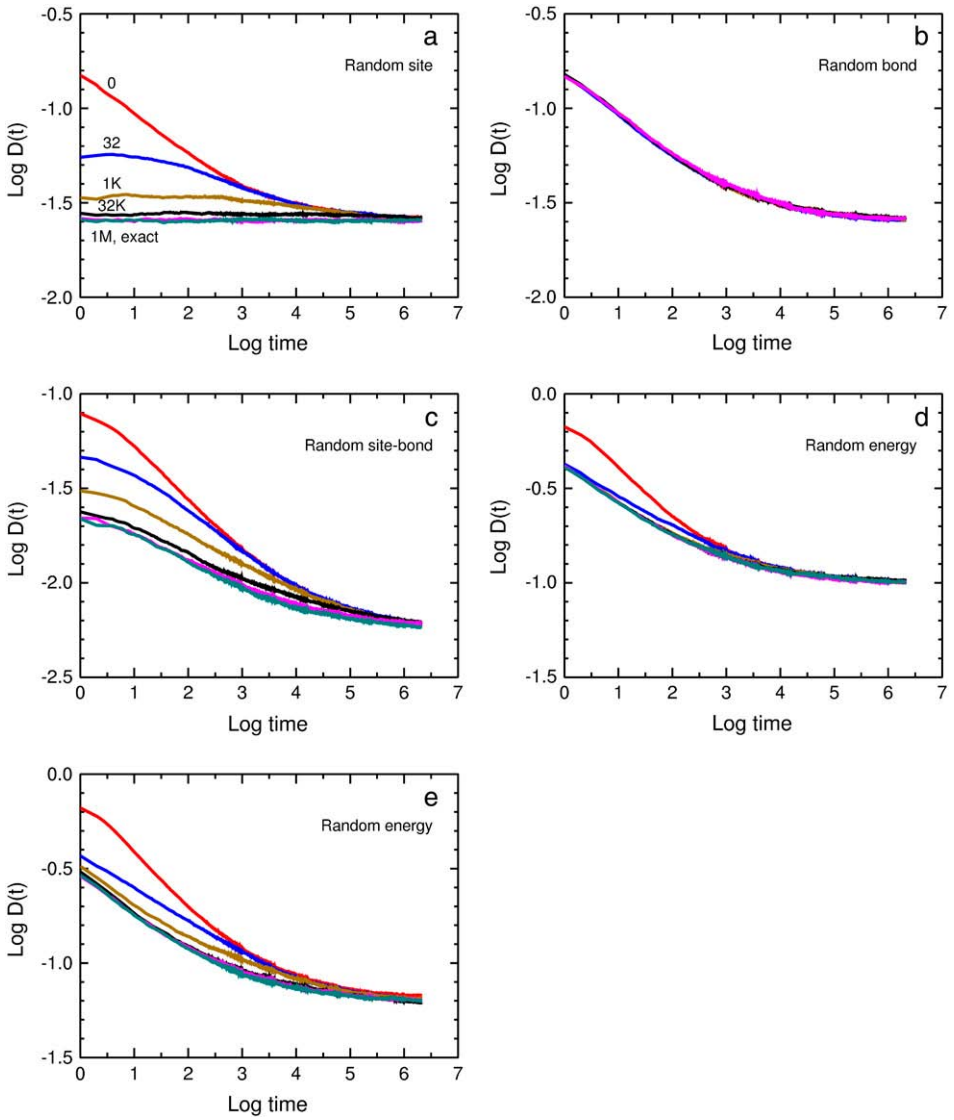

FIGURE 8 Effect of annealing time on a one-dimensional random walk for the different models. Annealing times are 0, 32, 1 K, 32 K, and 1 M; exact, from the equilibrium Boltzmann distribution. In panels *a–d*, 1000 lattice points were used, and in panel *e*, 3000 points. All sites or bonds were assigned random energies. The *y* axis is 1.5 units in all panels but shifted as required. (*a*) Random site model with a truncated Gaussian distribution of binding energies, mean 2.5, SD 1.5. (*b*) Random bond model, with the barrier heights from the same distribution. (*c*) Random site-bond model, with truncated Gaussian distributions of site energies and barrier heights, with mean 1.25 and SD 1.50. (*d*) Random energy model, with the same distribution of energies as the random site model. (*e*) Barbi random energy model with a nontruncated Gaussian distribution of site energies, mean −1.0 and SD 1.5. Barbi et al. (9,10) used the same mean and an SD ~2.5.

is nonuniform, there is no effect. Similarly, in a blind-ant random walk on a percolation cluster on a lattice, the equilibrium distribution of tracers is uniform and there is no annealing effect. In the blind-ant algorithm, at each time step the tracer tries to move to a randomly chosen nearest-neighbor site with equal probabilities, whether or not the sites are blocked. If the site is blocked, the tracer does not move but the clock is still incremented. Diffusion on an infinite percolation cluster is anomalous at all times, with $\alpha = 0.695$ in two and 0.515 in three dimensions (see ben-Avraham and Havlin, p. 79) (35).

In all four models, Gaussian distributions of energies are used with mean 2.5 and SD 1.5 for the random site, bond, and energy models, and mean 1.25, SD 1.5 for the random site-bond model. All energies are in units of kT. The Gaussian distributions are truncated to exclude negative values; well depths are then taken to be negative and barrier heights are taken to be positive. Other versions of these models in the literature restrict energies to positive values by using half-Gaussian, narrow full Gaussian, or exponential distributions. The system size is 1000. The Barbi model (9,10) of Fig. 8 *e* is a random energy model without truncation. Here the energies are Gaussian with mean −1 and SD 1.5, though the behavior is independent of the mean. The system size is 3000 and the initial position is chosen to be in [1000,1999] so there is a significant time in which the periodic boundary conditions have no effect. For easy comparison, the panels of Fig. 8 have the same interval on the *y*-axes, shifted as required.

Biological interpretation

A biological interpretation of a finite hierarchy of binding sites was inspired by experimental results of Platani et al. (4,11) on single-particle tracking of Cajal bodies in the

nucleus. In their experiments chromatin was labeled with a YFP-histone and the Cajal body marker protein coilin was labeled with GFP. The Cajal bodies alternated between association with chromatin and diffusion in the interchromatin space. Diffusion of Cajal bodies was anomalous, with $\alpha = 0.67$. ATP depletion and inhibition of transcription by actinomycin D increased the mobility and made diffusion less anomalous, as shown in Fig. 2 *a*. At the resolution of the measurements ATP depletion had no effect on chromatin structure. The authors' interpretation (4,11) is that Cajal bodies can be tethered to chromatin, and that tethering requires ATP and active transcription; an alternative interpretation is discussed later.

Consider the simplest picture of the results of Platani et al. (4). A Cajal body diffuses in the nucleus, interacts with various DNA sequences, and binds to some. It is plausible that there are many weak binding sites, corresponding to nonspecific binding sites. There is a single strongest binding site, corresponding to the target site for the Cajal body. There are a variety of intermediate binding sites, binding the Cajal body more or less strongly depending on how similar they are to the target site. So there is a hierarchy of binding energies resulting in a hierarchy of escape times. The simplest way to imagine this is in terms of a protein on the Cajal body looking for a particular sequence of basepairs, but the Cajal body could be examining higher-order structure in the DNA. Fig. 9 shows this interpretation in terms of Fig. 3.

In the cell the distribution of binding sites is presumably continuous, not discrete. But the transient anomalous subdiffusion found here for a discrete distribution in two dimensions (Fig. 4) and three dimensions (not shown) is similar to that found for continuous distributions in one dimension (Fig. 8, *a*, *c*, and *d*) and in two dimensions (5).

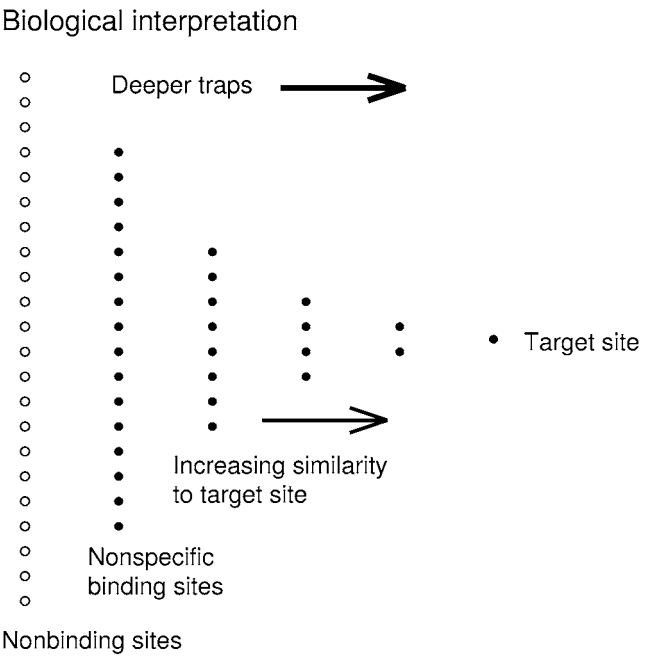

FIGURE 9 The biological interpretation of the hierarchy (see text). (*Open circles*) Nonbinding sites. (*Solid circles*) Binding sites with the binding growing stronger to the right.

Other assumptions

The model assumes that the traps are immobile; if they are not, their mobility must be taken into account. The model also assumes that reaction occurs when the diffusing species first reaches the target site. The target is assumed to be the deepest trap; in the example of Fig. 3, $P_{ESC} = 0.1$, so the escape time from the target is 10^5 time steps. The assumption is plausible but needs to be examined in applications.

Timescale

What is the timescale of the crossover? The timescale for a random walk on a lattice is arbitrary; one can choose any lattice constant ℓ and any time constant τ satisfying $\ell^2 = 2d D_0\tau$, where d is the dimensionality and D_0 is the diffusion coefficient in a system without traps. Escape times from traps are then expressed in terms of τ, and P_{ESC} is the probability of escape per time step τ. We must choose τ small enough to resolve the distribution of escape times.

The best choice for analyzing SPT data is probably to use the SPT resolution element (''resel'') as the length scale. (We call this an ''SPT resel'' to distinguish it from the ''confocal microscopy resel'', which is set by the Rayleigh length.) The SPT resel depends on the signal/noise ratio and other experimental details. Kubitscheck et al. (45) found a value of 30 nm for GTP in solution; values for membrane applications were 20–60 nm (46). For three-dimensional data the SPT resel has the complication that the resolution along the z axis is lower than that in the x,y plane.

So in the two-dimensional case one might choose ℓ to be a lipid diameter or a membrane protein diameter or an SPT resel size and find τ, or choose τ based on the video rate and find ℓ. For three-dimensional diffusion in the nucleus, one might choose ℓ to be the diameter of a protein or a chromatin fiber or a Cajal body or an SPT resel, or choose τ based on the video rate. For example, in the two-dimensional case, using the parameters from Saxton (2), we can take a lattice point to be a protein of diameter 4 nm with $D_0 = 3.75\ \mu m^2/s$ and obtain $\tau = 1.1\ \mu s$. A Monte Carlo crossover time of 50,000 as in Fig. 1 *c* would then yield a physical crossover time of 55 ms. Alternatively, we can use an SPT resel of, for example, $\ell = 20$ nm and $D = D(\text{lipid}) = 5\ \mu m^2/s$, giving $\tau = 20\ \mu s$ and a crossover time of 1 s.

Observability of traps

Can the trapping events responsible for anomalous subdiffusion be observed? FRAP is used extensively to detect binding (47–51), particularly of proteins in the nucleus. A limitation of FRAP is that it is at optical resolution, so,

depending on the density of traps in the particular system studied, it may be more suitable for measuring global anomalous subdiffusion than for resolving individual traps. The form of the recovery curve is known for normal diffusion (52) and for pure anomalous subdiffusion (18,53) but not for transient anomalous subdiffusion.

If the traps are far enough apart, FCS is promising. Jankevics et al. (54) used FCS to resolve classes of binding sites in the nucleus of living cells. In their diffusion-time distribution analysis, the maximum entropy method (55) was used to construct a histogram of the diffusion times of the estrogen receptor labeled with YFP. The diffusion times were in the range of 2–20 ms and were sensitive to agonists and antagonists. The histogram showed structure. The fastest motion was attributed to receptor dimers and receptors associated with chaperones; intermediate motion, to complexes of receptors with several cofactors; and the slowest motion, to receptors transiently interacting with chromatin or other nuclear structures. A new FCS technique measures the distance dependence of the diffusion coefficient by varying the laser spot size continuously. It has been applied to protein diffusion in hyaluronan solutions (56,57) and to corralled two-dimensional motion in membranes (58). This method could be useful in characterizing trapping sites; the radius of the smallest detectable corral was estimated to be 60 nm (58). If the identity of the binding site is known or suspected, useful approaches include cross correlation or image correlation FCS (59–62), fluorescence resonance energy transfer (63), and fluorescence brightness analysis using photon counting histograms (64).

If two requirements are met, single-particle tracking can resolve trapping events and permit measurement of escape times. First, the resolution of the SPT measurements must be sufficient. The resolution of two-color SPT is discussed in detail by Koyama-Honda et al. (65). Second, it is necessary to distinguish trapping events from the random periods of localized motion that are an inherent part of a pure random walk with no trapping or obstruction (66). Fig. 10 shows the square displacement r^2 as a function of time for random walks with and without trapping. The periods of trapping are clear in Fig. 10 *a*. Fig. 10 *b* shows random periods of localized motion in pure random walks. The difference is obvious here but noise in experimental trajectories could obscure the difference.

Individual trapping events did not appear in the plots of $\log \langle r^2 \rangle / t$ versus $\log t$ shown earlier. If P_{ESC} is small enough, say 0.01–0.02, discrete energy levels begin to appear. But for larger values of P_{ESC} they do not, for two reasons. First, the distribution of escape times is wide. If P is the escape probability for one time step and $Q = 1 - P$, then the probability of escape at the n^{th} time step is $f_{\mathrm{n}} = PQ^{\mathrm{n}-1}$, a modified geometric distribution. The mean escape time is $\langle n \rangle = 1/P$, and the SD is $\sqrt{1-P}/P$, so the ratio of the SD to the mean is $\sqrt{1-P} \approx 1$. Second, the structure disappears quickly on averaging, as shown in Fig. 10 *c*.

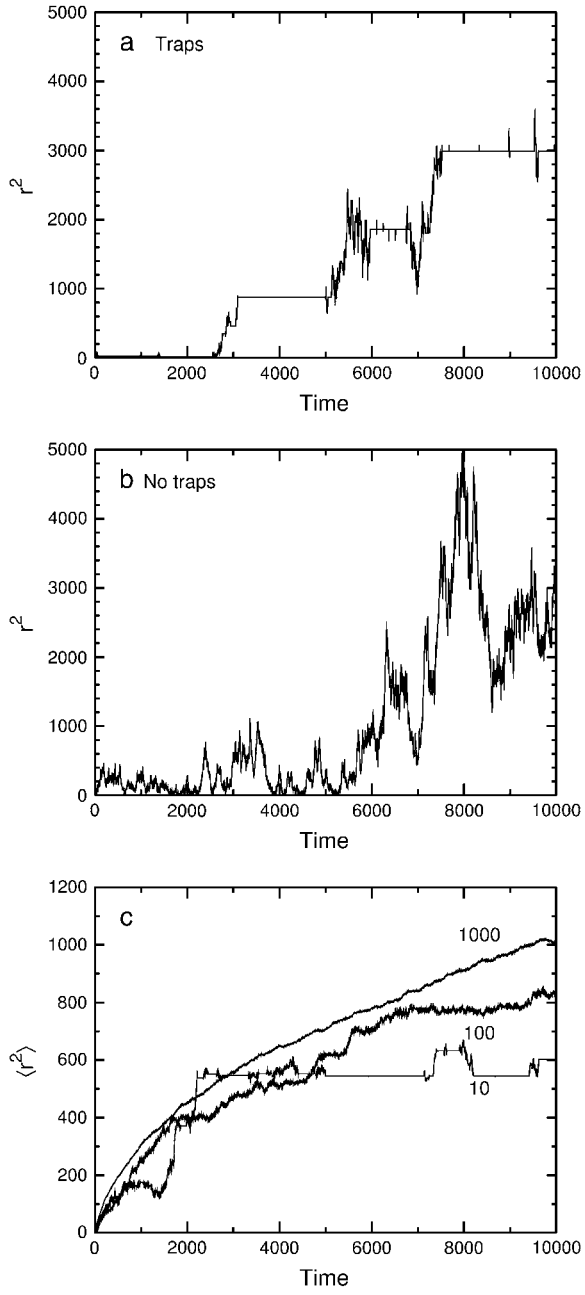

FIGURE 10 Observability of trapping. (*a*) Square displacement r^2 versus time t for a single random walk with trapping, assuming the standard hierarchy 16/8/4/2/− with $P_{\mathrm{ESC}} = 0.1$ and total trap concentration 0.02930. (*b*) The corresponding plot for a single pure random walk with no trapping or confinement. The curves in panels *a* and *b* were selected to make the point about the problem of apparent trapping, but they were selected from only five curves of each kind, and the problem is real. (*c*) Mean-square displacement $\langle r^2 \rangle$ averaged over 10, 100, and 1000 tracers for the same traps as in panel *a*.

DISCUSSION

We have proposed a model in which anomalous subdiffusion is inherently linked to metabolism. Some initial, energy-dependent biological event turns on the interaction of the diffusing species with a hierarchy of traps. The mobile species

diffuses and eventually reaches its target site, where it reacts or binds or signals. We interpret the abundant shallow traps of the hierarchy as nonspecific binding sites, the intermediate traps as traps with conformations more or less similar to the target site, and the deepest trap as the target site of the diffusing species. Intermediate traps are deeper the closer their conformation is to the conformation of the target site. The hierarchy is a sufficient condition for anomalous subdiffusion but not a necessary one. Diffusion can be briefly anomalous even with a single trap; the intermediate traps of a hierarchy lengthen the time during which anomalous subdiffusion occurs (Fig. 5). Diffusion becomes less anomalous as the diffusing particle equilibrates with the traps, and becomes purely normal at equilibrium. The equilibration shown in the Monte Carlo results of Figs. 6 and 8 *a* corresponds to the effect of ATP depletion in biological systems provided that ATP depletion does not also alter the structure of the system.

This picture holds for a pure binding site model. In a pure barrier model, anomalous subdiffusion may occur even at thermal equilibrium (Fig. 8 *b*). But in cells both binding sites and barriers are likely to be present, and the barriers are likely to be gates due to fluctuating macromolecules, not simply potential energy barriers. For example, in the Kusumi membrane skeleton picket fence model (12), the membrane skeleton acts as a barrier and transmembrane proteins may bind transiently to the membrane skeleton to form the fence pickets. In the nucleus, Cajal bodies are known to associate transiently with chromatin (67) and chromatin acts as a barrier to motion of Cajal bodies (4,68). When barriers and binding sites are present, the anomalous subdiffusion due to binding sites is removed by thermal equilibration but that due to barriers is not (Fig. 8 *c*). Indeed, Platani et al. (4) find that ATP depletion reduces but does not eliminate anomalous diffusion. This result is consistent with a binding site-barrier model, though it would be premature to claim agreement.

Understanding these results for the nucleus will require further work on chromatin dynamics, an active area of research (69–71). Platani et al. (4) found that at the resolution of their measurements ATP depletion had no effect on chromatin structure. Actinomycin D treatment, however, affected chromatin structure (see also (72)), suggesting that the increase in Cajal body mobility resulted from either disruption of chromatin structure or inhibition of transcription. Görisch et al. (68) proposed that nuclear bodies may diffuse rapidly within slowly mobile chromatin corrals. This idea was based on SPT measurements on Cajal bodies, promyelocytic leukemia (PML) bodies, and an artificial protein body. In this view ATP inhibition changes diffusion by changing the mobility and density of chromatin. The effect of actinomycin D was not examined.

The trap hierarchy model is potentially applicable to three-dimensional diffusion in the nucleus and cytoplasm, and to two-dimensional diffusion in membranes. All the mechanism requires is a stable particle small enough to undergo Brownian motion, a suitable distribution of traps, and a non-equilibrium state. Much work is being done on ways to characterize protein-protein and protein-nucleic acid interactions, both to study specific sets of interacting molecules and to identify the ''interactome,'' a genome-scale interaction map for the proteins in a cell (73). Among the methods are FRAP, FCS, SPT, two-hybrid measurements (74), molecular simulation (75), and data mining (76). It is important to recognize that the false positives found in these approaches are candidate intermediate binding sites in the hierarchy.

Interestingly, in one view of cell signaling, intermediate binding sites do not exist. Zarrinpar et al. (77,78) found that in one class of signaling proteins in yeast, selective pressure against cross talk has eliminated nonspecific binding sites for signaling proteins. Observations of diffusion in such a system would test this hypothesis, unfortunately not cleanly. The occurrence of anomalous subdiffusion would contradict the hypothesis but one would have to exclude crowding-induced anomalous subdiffusion (79,80) and anomalous subdiffusion due to barriers. The absence of anomalous subdiffusion could be the result of thermal equilibration or of the absence of intermediate binding sites.

A long-standing problem in membrane dynamics is the observation that diffusion in the plasma membrane is one or two orders of magnitude slower than diffusion of similar species reconstituted in vesicles (12,81). The reduction in diffusion coefficients due to high concentrations of mobile particles does not seem sufficient to account for this (81–84). Percolation, which is caused by immobile obstacles, seems unlikely to be the explanation because the obstacle concentration would have to be near the percolation threshold. But the threshold is defined as the excluded area fraction for each diffusing species, not as an area fraction of obstacles, so if the obstacles were at the threshold for small membrane proteins, they would be far from the threshold for either lipids or large membrane proteins. Transient binding seems an unlikely explanation because it would require universally sticky binding sites. A less specific mechanism is more plausible, combining obstruction and the hydrodynamic interaction of mobile particles with immobile obstacles, as proposed by Hammer, Koch, and collaborators (82–84). They found that the hydrodynamic effect is long-range and slightly greater than the obstruction effect. Immobile species have a much greater hydrodynamic effect than mobile species do; the same is true for the obstruction effect (85). The immobile obstacles would likely be transmembrane proteins bound to the cytoskeleton and forming the pickets of the Kusumi membrane skeleton fence model (12).

The traps in the hierarchy are more generic than in the simple examples given here. The mechanism is easiest to visualize and simulate in terms of protein-protein binding sites represented as point binding sites with a fixed escape probability per unit time. But what the mechanism actually

requires is an appropriate set of time delays. For example, in the nucleus one might have binding followed by one-dimensional diffusion along DNA to a release site, or mechanical trapping of a Cajal body in flexible chromatin fibers. In the plasma membrane the traps could involve partition into lipid domains or binding to domain interfaces. The binding of polystyrene beads to condensed lipid domains in monolayers and the diffusion of the beads along the interface was characterized by Selle et al. (86).

Barbi et al. (9,10) independently proposed a similar model for one-dimensional diffusion of a protein bound to DNA and searching for its target in an energy landscape. The interaction energy was modeled in terms of the differences in hydrogen bonding between the protein and the different DNA bases. The distribution of interaction energies was based on an actual DNA sequence or was assumed to be Gaussian. Their work suggests the intriguing possibility that their one-dimensional anomalous subdiffusion mechanism might provide a hierarchy of traps underlying larger-scale three-dimensional anomalous subdiffusion as described here. The main differences in the assumptions of the two models are that their model is one-dimensional and the simplest form of it is a random site/bond model. The results are somewhat different. Barbi et al. found no equilibration effect of the sort seen in Figs. 6 and 8, perhaps because the effect is difficult to see in log-log plots of mean-square displacement versus time. It is puzzling how they found a speedup of diffusion due to anomalous subdiffusion.

If the diffusing species is in equilibrium with the traps, diffusion is slow but normal at all times. Anomalous subdiffusion is thus probing the thermal equilibration of the cell. Obviously the cell and its membranes are at ambient or body temperature, and the internal degrees of freedom of the molecules are equilibrated. But a newly inserted protein in the plasma membrane or nucleus may be in a nonequilibrium state with respect to binding sites there. Nonequilibrium states could also result from conformational changes in the mobile species that changes its interaction with the traps. A trap-based nonequilibrium state results if the time delays are constantly changing, fast enough that the diffusing species cannot equilibrate with them. This would be a biological realization of the CTRW (87). Membrane corral fluctuations and ATP-dependent chromatin remodeling ought to be examined for this.

The model predicts that anomalous subdiffusion in cells requires metabolic energy. Experimental results are divided. For LDL receptors in fibroblasts (88) and Cajal bodies in the nucleus (4), yes. For IgE receptors in RBL cells (89), no. All three experiments used single-particle tracking. Further experiments would be of considerable interest.

I thank Jason Swedlow, Joan Ritland Politz, Silvia Cavagnero, Maria Barbi, and the reviewers for helpful comments.

This work was begun at the late Institute of Theoretical Dynamics, and was supported by National Institutes of Health grant No. GM038133.

REFERENCES

1. Stauffer, D., and A. Aharony. 1992. Introduction to Percolation Theory, 2nd Ed. Taylor & Francis, London.
2. Saxton, M. J. 1994. Anomalous diffusion due to obstacles: a Monte Carlo study. *Biophys. J.* 66:394–401.
3. Bouchaud, J. P., and A. Georges. 1990. Anomalous diffusion in disordered media. Statistical mechanisms, models and physical applications. *Phys. Rep.* 195:127–293.
4. Platani, M., I. Goldberg, A. I. Lamond, and J. R. Swedlow. 2002. Cajal body dynamics and association with chromatin are ATP-dependent. *Nat. Cell Biol.* 4:502–508.
5. Saxton, M. J. 1996. Anomalous diffusion due to binding: a Monte Carlo study. *Biophys. J.* 70:1250–1262.
6. Saxton, M. J. 2002. The biological meaning of anomalous subdiffusion. *Mol. Biol. Cell.* 13:275A.
7. Saxton, M. J. 2003. The biological meaning of anomalous subdiffusion. *Biophys. J.* 84:487A.
8. Saxton, M. J. 2004. A biological interpretation of anomalous subdiffusion. *Biophys. J.* 86:369A.
9. Barbi, M., C. Place, V. Popkov, and M. Salerno. 2004. Base-sequence-dependent sliding of proteins on DNA. *Phys. Rev. E.* 70:041901.
10. Barbi, M., C. Place, V. Popkov, and M. Salerno. 2004. A model of sequence-dependent protein diffusion along DNA. *J. Biol. Phys.* 30:203–226.
11. Platani, M., I. Goldberg, J. R. Swedlow, and A. I. Lamond. 2000. In vivo analysis of Cajal body movement, separation, and joining in live human cells. *J. Cell Biol.* 151:1561–1574.
12. Kusumi, A., C. Nakada, K. Ritchie, K. Murase, K. Suzuki, H. Murakoshi, R. S. Kasai, J. Kondo, and T. Fujiwara. 2005. Paradigm shift of the plasma membrane concept from the two-dimensional continuum fluid to the partitioned fluid: high-speed single-molecule tracking of membrane molecules. *Annu. Rev. Biophys. Biomolec. Struct.* 34:351–U54.
13. Murase, K., T. Fujiwara, Y. Umemura, K. Suzuki, R. Iino, H. Yamashita, M. Saito, H. Murakoshi, K. Ritchie, and A. Kusumi. 2004. Ultrafine membrane compartments for molecular diffusion as revealed by single molecule techniques. *Biophys. J.* 86:4075–4093.
14. Suzuki, K., K. Ritchie, E. Kajikawa, T. Fujiwara, and A. Kusumi. 2005. Rapid hop diffusion of a G-protein-coupled receptor in the plasma membrane as revealed by single-molecule techniques. *Biophys. J.* 88:3659–3680.
15. Morone, N., T. Fujiwara, K. Murase, R. S. Kasai, H. Ike, S. Yuasa, J. Usukura, and A. Kusumi. 2006. Three-dimensional reconstruction of the membrane skeleton at the plasma membrane interface by electron tomography. *J. Cell Biol.* 174:851–862.
16. Press, W. H., S. A. Teukolsky, W. T. Vetterling, and B. P. Flannery. 1992. Numerical Recipes in FORTRAN: The Art of Scientific Computing, 2nd Ed. Cambridge University Press, Cambridge. 272–273.
17. Saxton, M. J. 2007. Modeling two-dimensional and three-dimensional diffusion. *In* Methods in Membrane Lipids. A. Dopico, editor. Methods in Molecular Biology, Humana Press, Totowa, NJ. In press.
18. Saxton, M. J. 2001. Anomalous subdiffusion in fluorescence photobleaching recovery: a Monte Carlo study. *Biophys. J.* 81:2226–2240.
19. Harder, H., S. Havlin, and A. Bunde. 1987. Diffusion on fractals with singular waiting-time distribution. *Phys. Rev. B.* 36:3874–3879.
20. Bonfim, O. F. D., and M. Berrondo. 1989. Corrections to scaling for diffusion in disordered media. *J. Phys. A.* 22:4673–4679.
21. Shlesinger, M. F. 1988. Fractal time in condensed matter. *Annu. Rev. Phys. Chem.* 39:269–290.
22. Onuchic, J. N., and P. G. Wolynes. 2004. Theory of protein folding. *Curr. Opin. Struct. Biol.* 14:70–75.
23. Hanson, J. D., J. R. Cary, and J. D. Meiss. 1985. Algebraic decay in self-similar Markov chains. *J. Stat. Phys.* 39:327–345.
24. Giacometti, A., A. Maritan, and A. L. Stella. 1988. Diffusion on a one-dimensional structure with hierarchical waiting-time distribution. *Phys. Rev. B.* 38:2758–2764.

25. Huberman, B. A., and M. Kerszberg. 1985. Ultradiffusion: the relaxation of hierarchical systems. *J. Phys. A.* 18:L331–L336.
26. Maritan, A., and A. Stella. 1986. Exact renormalization group approach to ultradiffusion in a hierarchical structure. *J. Phys. A.* 19:L269–L273.
27. Teitel, S., D. Kutasov, and E. Domany. 1987. Diffusion and dynamical transition in hierarchical systems. *Phys. Rev. B.* 36:684–698.
28. Havlin, S., and H. Weissman. 1988. Anomalous logarithmic slow dynamics behavior on hierarchical and random systems. *Phys. Rev. B.* 37:487–491.
29. Metzler, R., and J. Klafter. 2000. Subdiffusive transport close to thermal equilibrium: from the Langevin equation to fractional diffusion. *Phys. Rev. E.* 61:6308–6311.
30. Scher, H., M. F. Shlesinger, and J. T. Bendler. Jan. 1991. Timescale invariance in transport and relaxation. *Phys. Today.* 44:26–34.
31. Haus, J. W., K. W. Kehr, and J. W. Lyklema. 1982. Diffusion in a disordered medium. *Phys. Rev. B.* 25:2905–2907.
32. Haus, J. W., and K. W. Kehr. 1987. Diffusion in regular and disordered lattices. *Phys. Rep.* 150:263–406.
33. Kehr, K. W., and T. Wichmann. 1996. Diffusion coefficients of single and many particles in lattices with different forms of disorder. *Mater. Sci. Forum.* 223–224:151–160.
34. Van Beijeren, H., K. W. Kehr, and R. Kutner. 1983. Diffusion in concentrated lattice gases. 3. Tracer diffusion on a one-dimensional lattice. *Phys. Rev. B.* 28:5711–5723.
35. ben-Avraham, D., and S. Havlin. 2000. Diffusion and Reactions in Fractals and Disordered Systems. Cambridge University Press, Cambridge.
36. Alexander, S., J. Bernasconi, W. R. Schneider, and R. Orbach. 1981. Excitation dynamics in random one-dimensional systems. *Revs. Mod. Phys.* 53:175–198.
37. Havlin, S., and D. Ben-Avraham. 1987. Diffusion in disordered media. *Adv. Phys.* 36:695–798.
38. Berlin, Y. A., and A. L. Burin. 1996. Diffusion in one-dimensional disordered systems. *Chem. Phys. Lett.* 257:665–673.
39. Berlin, Y. A., L. D. A. Siebbeles, and A. A. Zharikov. 1997. Thermally activated diffusion along one-dimensional chains with energetic disorder: analysis of computer simulation data. *Chem. Phys. Lett.* 276: 361–370.
40. Argyrakis, P., A. Milchev, V. Pereyra, and K. W. Kehr. 1995. Dependence of the diffusion coefficient on the energy distribution of random barriers. *Phys. Rev. E.* 52:3623–3631.
41. Avramov, I., A. Milchev, and P. Argyrakis. 1993. Diffusion in a random medium: a Monte Carlo study. *Phys. Rev. E.* 47:2303–2307.
42. Horner, A., A. Milchev, and P. Argyrakis. 1995. Role of percolation in diffusion on random lattices. *Phys. Rev. E.* 52:3570–3576.
43. Limoge, Y., and J. L. Bocquet. 1990. Temperature behavior of tracer diffusion in amorphous materials: a random-walk approach. *Phys. Rev. Lett.* 65:60–63.
44. Mussawisade, K., T. Wichmann, and K. W. Kehr. 1997. Combination of random-barrier and random-trap models. *J. Phys. Cond. Mat.* 9: 1181–1189.
45. Kubitscheck, U., O. Kuckmann, T. Kues, and R. Peters. 2000. Imaging and tracking of single GFP molecules in solution. *Biophys. J.* 78:2170–2179.
46. Lagerholm, B. C., G. E. Weinreb, K. Jacobson, and N. L. Thompson. 2005. Detecting microdomains in intact cell membranes. *Annu. Rev. Phys. Chem.* 56:309–336.
47. Carrero, G., E. Crawford, J. Th'ng, G. De Vries, and M. J. Hendzel. 2004. Quantification of protein-protein and protein-DNA interactions in vivo, using fluorescence recovery after photobleaching. *Meth. Enzymol.* 375:415–442.
48. Phair, R. D., P. Scaffidi, C. Elbi, J. Vecerova, A. Dey, K. Ozato, D. T. Brown, G. Hager, M. Bustin, and T. Misteli. 2004. Global nature of dynamic protein-chromatin interactions in vivo: three-dimensional genome scanning and dynamic interaction networks of chromatin proteins. *Mol. Cell. Biol.* 24:6393–6402.
49. Phair, R. D., S. A. Gorski, and T. Misteli. 2004. Measurement of dynamic protein binding to chromatin in vivo, using photobleaching microscopy. *Meth. Enzymol.* 375:393–414.
50. Sprague, B. L., R. L. Pego, D. A. Stavreva, and J. G. McNally. 2004. Analysis of binding reactions by fluorescence recovery after photobleaching. *Biophys. J.* 86:3473–3495.
51. Sprague, B. L., and J. G. McNally. 2005. FRAP analysis of binding: proper and fitting. *Trends Cell Biol.* 15:84–91.
52. Axelrod, D., D. E. Koppel, J. Schlessinger, E. Elson, and W. W. Webb. 1976. Mobility measurement by analysis of fluorescence photobleaching recovery kinetics. *Biophys. J.* 16:1055–1069.
53. Glöckle, W. G., T. Mattfeldt, and T. F. Nonnenmacher. 1994. Anomalous diffusion and angle-dependency in the theory of fluorescence recovery after photobleaching. *In* Fractals in Biology and Medicine. T. F. Nonnenmacher, G. A. Losa, and E. R. Weibel, editors. Birkhäuser Verlag, Basel. 363–371.
54. Jankevics, H., M. Prummer, P. Izewska, H. Pick, K. Leufgen, and H. Vogel. 2005. Diffusion-time distribution analysis reveals characteristic ligand-dependent interaction patterns of nuclear receptors in living cells. *Biochemistry.* 44:11676–11683.
55. Sengupta, P., K. Garai, J. Balaji, N. Periasamy, and S. Maiti. 2003. Measuring size distribution in highly heterogeneous systems with fluorescence correlation spectroscopy. *Biophys. J.* 84:1977–1984.
56. Masuda, A., K. Ushida, and T. Okamoto. 2005. Direct observation of spatiotemporal dependence of anomalous diffusion in inhomogeneous fluid by sampling-volume-controlled fluorescence correlation spectroscopy. *Phys. Rev. E.* 72:060101.
57. Masuda, A., K. Ushida, and T. O. Riken. 2005. New fluorescence correlation spectroscopy enabling direct observation of spatiotemporal dependence of diffusion constants as an evidence of anomalous transport in extracellular matrices. *Biophys. J.* 88:3584–3591.
58. Wawrezinieck, L., H. Rigneault, D. Marguet, and P. F. Lenne. 2005. Fluorescence correlation spectroscopy diffusion laws to probe the submicron cell membrane organization. *Biophys. J.* 89:4029–4042.
59. Bacia, K., and P. Schwille. 2003. A dynamic view of cellular processes by in vivo fluorescence auto- and cross-correlation spectroscopy. *Methods.* 29:74–85.
60. Digman, M. A., P. Sengupta, P. W. Wiseman, C. M. Brown, A. R. Horwitz, and E. Gratton. 2005. Fluctuation correlation spectroscopy with a laser-scanning microscope: exploiting the hidden time structure. *Biophys. J.* 88:L33–L36.
61. Larson, D. R., J. A. Gosse, D. A. Holowka, B. A. Baird, and W. W. Webb. 2005. Temporally resolved interactions between antigen-stimulated IgE receptors and Lyn kinase on living cells. *J. Cell Biol.* 171:527–536.
62. Nohe, A., and N. O. Petersen. 2004. Analyzing protein-protein interactions in cell membranes. *BioEssays.* 26:196–203.
63. Day, R. N., A. Periasamy, and F. Schaufele. 2001. Fluorescence resonance energy transfer microscopy of localized protein interactions in the living cell nucleus. *Methods.* 25:4–18.
64. Chen, Y., L. N. Wei, and J. D. Muller. 2005. Unraveling protein-protein interactions in living cells with fluorescence fluctuation brightness analysis. *Biophys. J.* 88:4366–4377.
65. Koyama-Honda, I., K. Ritchie, T. Fujiwara, R. Iino, H. Murakoshi, R. S. Kasai, and A. Kusumi. 2005. Fluorescence imaging for monitoring the colocalization of two single molecules in living cells. *Biophys. J.* 88:2126–2136.
66. Saxton, M. J. 1993. Lateral diffusion in an archipelago: single-particle diffusion. *Biophys. J.* 64:1766–1780.
67. Swedlow, J. R., and A. I. Lamond. 2001. Nuclear dynamics: where genes are and how they got there. *Genome Biol.* 2:0002.1–0002.7.
68. Görisch, S. M., M. Wachsmuth, C. Ittrich, C. P. Bacher, K. Rippe, and P. Lichter. 2004. Nuclear body movement is determined by chromatin accessibility and dynamics. *Proc. Natl. Acad. Sci. USA.* 101:13221–13226.
69. Bacher, C. P., M. Reichenzeller, C. Athale, H. Herrmann, and R. Eils. 2004. 4-D single particle tracking of synthetic and proteinaceous

microspheres reveals preferential movement of nuclear particles along chromatin-poor tracks. *BMC Cell Biol.* 5:45.

70. Levi, V., Q. Q. Ruan, M. Plutz, A. S. Belmont, and E. Gratton. 2005. Chromatin dynamics in interphase cells revealed by tracking in a two-photon excitation microscope. *Biophys. J.* 89:4275–4285.
71. Shav-Tal, Y., X. Darzacq, S. M. Shenoy, D. Fusco, S. M. Janicki, D. L. Spector, and R. H. Singer. 2004. Dynamics of single mRNPs in nuclei of living cells. *Science.* 304:1797–1800.
72. Nickerson, J. A., G. Krochmalnic, K. M. Wan, and S. Penman. 1989. Chromatin architecture and nuclear RNA. *Proc. Natl. Acad. Sci. USA.* 86:177–181.
73. Ramani, A. K., R. C. Bunescu, R. J. Mooney, and E. M. Marcotte. 2005. Consolidating the set of known human protein-protein interactions in preparation for large-scale mapping of the human interactome. *Genome Biol.* 6:R40.1–R40.12.
74. Piehler, J. 2005. New methodologies for measuring protein interactions in vivo and in vitro. *Curr. Opin. Struct. Biol.* 15:4–14.
75. Deremble, C., and R. Lavery. 2005. Macromolecular recognition. *Curr. Opin. Struct. Biol.* 15:171–175.
76. Miller, J. P., R. S. Lo, A. Ben-Hur, C. Desmarais, I. Stagljar, W. S. Noble, and S. Fields. 2005. Large-scale identification of yeast integral membrane protein interactions. *Proc. Natl. Acad. Sci. USA.* 102:12123–12128.
77. Zarrinpar, A., S. H. Park, and W. A. Lim. 2003. Optimization of specificity in a cellular protein interaction network by negative selection. *Nature.* 426:676–680.
78. Endy, D., and M. B. Yaffe. 2003. Signal transduction: molecular monogamy. *Nature.* 426:614–615.
79. Banks, D. S., and C. Fradin. 2005. Anomalous diffusion of proteins due to molecular crowding. *Biophys. J.* 89:2960–2971.
80. Weiss, M., M. Elsner, F. Kartberg, and T. Nilsson. 2004. Anomalous subdiffusion is a measure for cytoplasmic crowding in living cells. *Biophys. J.* 87:3518–3524.
81. Saxton, M. J. 1999. Lateral diffusion of lipids and proteins. *Curr. Topics Membr.* 48:229–282.
82. Bussell, S. J., D. L. Koch, and D. A. Hammer. 1995. Effect of hydrodynamic interactions on the diffusion of integral membrane proteins: tracer diffusion in organelle and reconstituted membranes. *Biophys. J.* 68:1828–1835.
83. Bussell, S. J., D. L. Koch, and D. A. Hammer. 1995. Effect of hydrodynamic interactions on the diffusion of integral membrane proteins: diffusion in plasma membranes. *Biophys. J.* 68:1836–1849.
84. Dodd, T. L., D. A. Hammer, A. S. Sangani, and D. L. Koch. 1995. Numerical simulations of the effect of hydrodynamic interactions on diffusivities of integral membrane proteins. *J. Fluid Mech.* 293: 147–180.
85. Saxton, M. J. 1990. Lateral diffusion in a mixture of mobile and immobile particles: a Monte Carlo study. *Biophys. J.* 58:1303–1306.
86. Selle, C., F. Ruckerl, D. S. Martin, M. B. Forstner, and J. A. Käs. 2004. Measurement of diffusion in Langmuir monolayers by single-particle tracking. *Phys. Chem. Chem. Phys.* 6:5535–5542.
87. Feder, T. J., I. Brust-Mascher, J. P. Slattery, B. Baird, and W. W. Webb. 1996. Constrained diffusion or immobile fraction on cell surfaces: a new interpretation. *Biophys. J.* 70:2767–2773.
88. Ghosh, R. N. 1991. Mobility and clustering of individual low-density lipoprotein receptor molecules on the surface of human skin fibroblasts. PhD thesis, Cornell University, Ithaca, NY.
89. Slattery, J. P. 1995. Lateral mobility of FcεRI on rat basophilic leukemia cells as measured by single particle tracking using a novel bright fluorescent probe. PhD thesis, Cornell University, Ithaca, NY.